Electron-Paramagnetic-Resonance Spectra of Nd^{3+}, Dy^{3+}, Er^{3+}, and Yb^{3+} in Lithium Yttrium Fluoride

J. P. Sattler and J. Nemarich

Harry Diamond Laboratories, Washington, D. C. 20438

The electron-paramagnetic-resonance spectra have been obtained for trivalent neodymium, dysprosium, erbium, and ytterbium in single-crystal samples of the scheelite lithium yttrium fluoride. The measurements were made at X-band frequencies and at 4.2 °K. The ions were found to have axial spectra which, together with chemical arguments, indicate that they occupy Y^{3+} sites with S_4 point symmetry. g factors and hyperfine parameters were obtained by the complete diagonalization of the spin Hamiltonian and least-squares fitting to the observed spectra. The ground-state irreducible representations for Yb^{3+} and Nd^{3+} were determined to be $\Gamma_{5,6}$ and $\Gamma_{7,8}$, respectively. Superhyperfine structure was observed in the Yb^{3+} c-axis spectrum.

I. INTRODUCTION

There has been considerable interest in the electron paramagnetic resonance (EPR) and optical spectra of rare-earth ions in the tungstate and molybdate crystals with scheelite ($CaWO_4$) structure.[1-5] These crystals vary approximately 30% in unit-cell volume, and may be grown with up to several percent rare-earth impurity. The rare-earth ions substitute for divalent cations which have tetragonal (S_4) symmetry. By doping a series of scheelites with a rare-earth ion, the surroundings of the ionic impurity may be varied while preserving the tetragonal point symmetry. This family of crystals has therefore been recognized as useful for investigating the crystal-field model.

Lithium yttrium fluoride also possesses scheelite structure[6] and should prove to be an interesting host for the study of the spectra of rare-earth ions. On the basis of the similarity of ionic radii and the chemical properties of yttrium and rare-earth ions, it is expected that trivalent rare-earth ions will substitute for trivalent yttrium[7,8] ions which have tetragonal (S_4) symmetry. This substitution of a rare-earth ion for an ion with the same valence is to be contrasted with the tungstate and molybdate scheelites where the rare-earth ion substitutes for the divalent cations of calcium, strontium, etc. The result should be less disruption of the host lattice by the impurity ion in $LiYF_4$. Comparison of

the optical spectra of neodymium in $CaWO_4$ and $LiYF_4$ appears to bear out this conjecture.[7] In addition, since $LiYF_4$ is probably more nearly an ionic crystal than the tungstate and molybdate scheelites, it should allow a more realistic comparison of experimental crystal-field parameters with those calculated from a point-charge model.

In this paper we report on the EPR spectra of Nd^{3+}, Dy^{3+}, Er^{3+}, and Yb^{3+} in samples of single crystal $LiYF_4$. The results are compared with those previously published for these ions in tungstate and molybdate scheelites. An axial resonance spectrum was observed for each ion, and g factors and hyperfine parameters were obtained by fitting to an axial spin Hamiltonian. Superhyperfine structure (SHFS) was observed on the Yb^{3+} spectrum, when the external field was parallel to the crystal c axis. The similarity of the SHFS to that reported for Yb^{3+} in CaF_2 suggests that the effect is due to the nuclear magnetic moments of the ligand fluorine ions.[9]

II. CRYSTAL STRUCTURE OF $LiYF_4$

The scheelite structure of $LiYF_4$ was determined by Thoma *et al.*[6] using x-ray diffraction. One may take $CaWO_4$ as the prototype crystal for the scheelite family which has the space group classification C_{4h}^6 ($I4_1/a$). With respect to the $CaWO_4$ unit cell, in $LiYF_4$, yttrium is at the calcium site, lithium is at the tungsten site, and fluorine is at the oxygen

TABLE I. Lattice parameters for several crystals with scheelite structure.

Crystal	c(Å)	a(Å)	c/a
LiYF$_4$ (Ref. 6)	10.94(3)	5.26(3)	2.08
LiYF$_4$ (Ref. 10)	10.85(3)	5.16(1)	2.10
CdMoO$_4$ (Ref. 11)	11.194	5.1554	2.171
CaWO$_4$ (Ref. 12)	11.376(3)	5.243(2)	2.170
PbMoO$_4$ (Ref. 13)	12.0165(39)	5.4312(16)	2.212
BaWO$_4$ (Ref. 11)	12.720	5.6134	2.266

site. The lattice parameters for LiYF$_4$ and several other scheelites are shown in Table I. The tungstates and molybdates listed span the range of lattice sizes for scheelites that have been commonly used as hosts for rare-earth ions. The quantity c represents the length of the unique axis of the tetragonal body-centered unit cell, and a is the length of a base side. From the comparison with other scheelites, one sees that LiYF$_4$ has a smaller c-axis length, and a lower c/a ratio.

III. EXPERIMENTAL DETAILS

The measurements were made at 4.2 °K with an X-band superheterodyne EPR spectrometer operating in the absorption mode. The rectangular sample cavity was designed so that crystals mounted in it could be rotated in a vertical plane while they were still immersed in liquid helium. Using this device, and a magnet mounted on a calibrated rotatable horizontal base, the angle between the c axis and the magnetic field could be determined to a tenth of a degree.

The crystal samples were grown by Linz and Gabbe of MIT, and Farrar of Harry Diamond Laboratories (HDL).

The LiYF$_4$:Yb sample had a 0.1-at.% ytterbium doping and the LiYF$_4$:Nd sample had a 2-at.% neodymium doping in the melt. A sample with a melt concentration of 2-at.% erbium had such a broad EPR line that the hyperfine structure could not be distinguished. From this, one is tempted to conclude that erbium doping can be achieved more readily than neodymium doping.

The LiYF$_4$ crystals grown at this laboratory were pulled from the melt in an a-axis direction. The boule cross sections were elliptical in shape with the c axis parallel to the major axis. For CaWO$_4$ and other scheelites, the c axis was parallel to the minor axis.[14]

The EPR spectra of Er^{3+} and Dy^{3+} were first discovered and measured in a LiYF$_4$ sample which had been grown without intentional rare-earth doping. The trace amounts of Er^{3+} and Dy^{3+} had probably been present as impurities in the yttrium fluoride starting material. These ions were identified from their hyperfine structure. The identification was checked by measuring spectra in intentionally doped crystals. It was found that the resolution of the hyperfine lines was better in the "undoped" LiYF$_4$, so this crystal was used to measure the hyperfine parameters.

Several other resonance lines have been noted in every LiYF$_4$ sample so far examined, but these lines have not yet been identified.

IV. ANALYSIS

The spin Hamiltonian used to fit the data was

$$\mathcal{H} = g_{\parallel}\mu_B H_z S_z + g_{\perp}\mu_P(H_x S_x + H_y S_y) + A I_z S_z$$

$$+ B(I_x S_x + I_y S_y) + P[I_z^2 - \tfrac{1}{3}I(I+1)] . \quad (1)$$

Here $S = \tfrac{1}{2}$ for these Kramers ions, and the quantity I takes on appropriate values for the various isotopes. Least-squares fit spin-Hamiltonian parameters were calculated by computer using an iterative procedure which included complete diagonalization of the spin Hamiltonian. The results are given in Table II. Also listed are the measured peak-to-trough derivative linewidths $\Delta H_{\parallel}$ and $\Delta H_{\perp}$ for the parallel and perpendicular spectra. (The quantity $\Delta H_{\perp}$ is not necessarily constant for every perpendicular direction.)

TABLE II. Spin-Hamiltonian parameters for rare-earth ions in LiYF$_4$.

Ion	$g_{\parallel}$	$g_{\perp}$	$\Delta H_{\parallel}$ (G)	$\Delta H_{\perp}$ (G)	Isotope	A (10^{-4} cm^{-1})	B (10^{-4} cm^{-1})	P (10^{-4} cm^{-1})
Nd^{3+}	1.987(2)	2.554(3)	18.8	25.1	143	197(6)	263(9)	...
					145	124(4)	164(6)	...
Dy^{3+}	1.112(2)	9.219(15)	8.2	10.9	161	31.6(8)	263(5)	<30
					163	41.5(10)	366(3)	<40
Er^{3+}	3.137(3)	8.105(12)	13.2	11.3	167	108.6(6)	280(3)	...
	3.32(1)[a]	8.09(5)[a]						
Yb^{3+}	1.3308(6)	3.917(3)	19.7	13.9	171	338(2)	1028(4)	...
					173	92.5(5)	284(1)	...

[a]Reference 8.

The rms deviation between a measured and calculated line position was less than one-fifth of a linewidth for all spectra except the parallel spectrum of Dy^{3+}. The rms deviation was just slightly less than the average measured linewidth for Dy^{3+}. It is not known why the fit was not better, but it may be that a spin Hamiltonian with higher terms than those in Eq. (1) is required to describe adequately the spectrum. A quadrupole term was needed only for Dy^{3+}.

The difference between the value of $g_{\parallel}$ for Er^{3+} reported here and in Ref. 8 may be due in part to the higher concentration of erbium in the samples used in Ref. 8.

V. DISCUSSION

Arguments have been presented which indicate that trivalent rare-earth ions substitute for the divalent cations in the tungstate and molybdate scheelites.[4,14,15] Similar considerations of crystal structure, valence, ionic size, and the axial symmetry of the EPR resonances indicate that the rare-earth ions are located at the yttrium site of S_4 point symmetry in $LiYF_4$. These arguments are strengthened by the fact that no charge compensation is necessary in this case. The crystal structure is too compact[16] for interstitial sites which, moreover, would not have axial resonance spectra. The lithium and yttrium sites alone have tetragonal symmetry. Trivalent rare earths, with ionic radii ranging from 1.28 to 1.12 Å would be expected to substitute for the trivalent yttrium ion of radius 1.115 Å rather than the smaller univalent lithium ion of radius 0.73 Å.[17]

The EPR data may be used to determine the S_4 irreducible representations of the ground states for Yb^{3+} and Nd^{3+}. As discussed in Ref. 4, the ground-state g factors for Yb^{3+} are related by

$$4g_{\perp}^2 = -3g_{\parallel}^2 + 6\Lambda g_{\parallel} + 45\Lambda^2 \ ,$$

if the state is characterized by $J = \frac{7}{2}$ with Kramers components

$$| \Gamma_5 \rangle = a | \tfrac{7}{2}, \tfrac{5}{2} \rangle + b | \tfrac{7}{2}, -\tfrac{3}{2} \rangle \ ,$$

$$| \Gamma_6 \rangle = -a^* | \tfrac{7}{2}, -\tfrac{5}{2} \rangle - b^* | \tfrac{7}{2}, \tfrac{3}{2} \rangle \ .$$

Here the states are expressed in $| JM \rangle$ notation and $\Lambda = \frac{8}{7}$ is the Landé factor for the $^2F_{7/2}$ multiplet of Yb^{3+}. The corresponding relationship is

$$4g_{\perp}^2 = g_{\parallel}^2 + 14\Lambda g_{\parallel} + 49\Lambda^2$$

for a pure $J = \frac{7}{2}$, $\Gamma_{7,8}$ state with components

$$| \Gamma_7 \rangle = c | \tfrac{7}{2}, \tfrac{1}{2} \rangle + d | \tfrac{7}{2}, -\tfrac{7}{2} \rangle \ ,$$

$$| \Gamma_8 \rangle = -c^* | \tfrac{7}{2}, -\tfrac{1}{2} \rangle - d^* | \tfrac{7}{2}, \tfrac{7}{2} \rangle \ .$$

The degree of J mixing is small[18] and can be neglected for the purpose of determining the ground state. This is also evident from the fact that the Elliott-Stevens parameter[19] $\alpha = A g_{\perp}/B g_{\parallel}$ is approximately unity. The measured g factors fit the relation for the $\Gamma_{5,6}$ state more closely, and so we make this assignment for the ground state of Yb^{3+}. This is consistent with the optical analysis of $LiYF_4 : Yb^{3+}$.[18]

The ground state for the $^4I_{9/2}$ multiplet of Nd^{3+} may have the components

$$| \Gamma_5 \rangle = a | \tfrac{9}{2}, \tfrac{5}{2} \rangle + b | \tfrac{9}{2}, -\tfrac{3}{2} \rangle \ ,$$

$$| \Gamma_6 \rangle = -a^* | \tfrac{9}{2}, -\tfrac{5}{2} \rangle - b^* | \tfrac{9}{2}, \tfrac{3}{2} \rangle$$

or the components

$$| \Gamma_7 \rangle = a | \tfrac{9}{2}, \tfrac{9}{2} \rangle + b | \tfrac{9}{2}, \tfrac{1}{2} \rangle + c | \tfrac{9}{2}, -\tfrac{7}{2} \rangle,$$

$$| \Gamma_8 \rangle = -a^* | \tfrac{9}{2}, -\tfrac{9}{2} \rangle - b^* | \tfrac{9}{2}, -\tfrac{1}{2} \rangle - c^* | \tfrac{9}{2}, \tfrac{7}{2} \rangle,$$

if the effects of J mixing are neglected. The Elliott-Stevens parameter α is about 0.96 for $LiYF_4 : Nd$, so we shall neglect J mixing. It may be readily shown that the g factors are related by

$$16g_{\perp}^2 = 21(-g_{\parallel}^2 + 2\Lambda g_{\parallel} + 15\Lambda^2) \ ,$$

if the ground state is a $\Gamma_{5,6}$. Here $\Lambda = \frac{8}{11}$ is the Landé factor for the $J = \frac{9}{2}$ multiplet of Nd^{3+}. Since the measured g factors do not satisfy this equation, the ground state is assigned as a $\Gamma_{7,8}$, even though the EPR data are not enough to determine the wave function uniquely. This assignment is consistent with the optical analysis.[20]

TABLE III. g factors for rare-earth ions in scheelite crystals.

Crystals	Nd^{3+}		Dy^{3+}		Er^{3+}		Yb^{3+}	
	$g_{\parallel}$	$g_{\perp}$	$g_{\parallel}$	$g_{\perp}$	$g_{\parallel}$	$g_{\perp}$	$g_{\parallel}$	$g_{\perp}$
LiYF$_4$	1.987[a]	2.554[a]	1.112[a]	9.219[a]	3.137[a]	8.105[a]	1.3308[a]	3.917[a]
CdMoO$_4$	2.302[b]	2.492[b]	...	...	...	...	1.2393[c]	3.917[c]
CaWO$_4$	2.035[b]	2.537[b]	7.5[d]	5.5[d]	1.247[e]	8.38[e]	1.0530[c]	3.916[c]
PbMoO$_4$	1.351[b]	2.592[b]	...	...	1.195[e]	8.45[e]	0.6622[c]	3.883[c]
BaWO$_4$	0.820[b]	2.563[b]	...	...	1.164[e]	8.62[e]	0.234[c]	3.822[c]

[a]Present results.   [b]Reference 22.   [c]Reference 4.   [d]Reference 23.   [e]Reference 21.

LiYF$_4$: Yb(0.1%)

H ‖ [001]

4.2° K

5007.6G   4924.8G
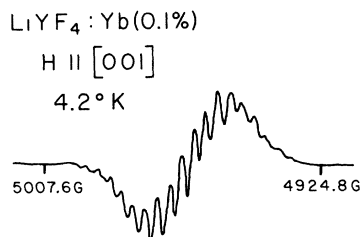
FIG. 1. Superhyperfine structure on EPR resonance
line of $I = 0$ Yb^{3+} in LiYF$_4$.

The irreducible representations of the ground
states of Dy^{3+} and Er^{3+} could not be determined
from the EPR results. Both ions have ground mul-
tiplets with $J = \frac{15}{2}$ and therefore have four projections
possible in each of the Kramers components of
either the $\Gamma_{5,6}$ or the $\Gamma_{7,8}$ ground states for H paral-
lel to c. Hence the values of $g_{\parallel}$ and $g_{\perp}$ alone are
insufficient, in general, to allow one to distinguish
between the two possible irreducible representa-
tions.

It is instructive to compare the g factors for
these ions in several scheelite crystals. Table III
gives the ground-state g factors in LiYF$_4$, CdMoO$_4$,
CaWO$_4$, PbMoO$_4$, and BaWO$_4$ for the rare-earth
ions Nd^{3+}, Dy^{3+}, Er^{3+}, and Yb^{3+}. Previous
studies[4,21,22] of the tungstate and molybdate schee-
lites have noted that an approximately linear re-
lationship between the g factors and c-axis lattice
parameter holds for the ions Yb^{3+}, Er^{3+}, and Nd^{3+}.
The reason for this dependence has not yet been
demonstrated. The g factors depend on wave-func-
tion coefficients which may be evaluated explicitly
in terms of the crystal-field parameters, which
themselves depend on sums over the ions in the lat-
tice. There is no *a priori* reason why the g factors
should have a linear dependence on the c-axis lat-
tice parameter, and breakdown of this empirical
relationship should not be regarded as surprising,
particularly if one goes from oxygen to fluorine co-
ordination. Using the data in Tables I and III, one
can show that this linear relationship holds for
LiYF$_4$: Yb, begins to break down for LiYF$_4$: Nd,
and breaks down entirely for LiYF$_4$: Er. The EPR
of Dy^{3+} has been reported previously in scheelites
for only CaWO$_4$: Dy,[23] and so one cannot establish a
trend for this ion. It is apparent, however, that
the g factors of Dy^{3+} in CaWO$_4$ and LiYF$_4$ are very
different. Karayianis has pointed out that for two
levels of the same representation, the sensitivity

of the g factors to changes in the crystal-field
parameters increases as their energy separation
decreases.[24] The two lowest levels with the same
irreducible representations are separated by about
132 cm^{-1} for Nd^{3+} in LiYF$_4$,[7] about 17 cm^{-1} for Er^{3+}
in LiYF$_4$,[8] and about 425 cm^{-1} for Yb^{3+} in LiYF$_4$.[18]
The separations are not significantly different for
these ions in CaWO$_4$. The spectrum of Dy^{3+} in
scheelites has been obtained only in CaWO$_4$, and
there are two excited levels within less than 10
cm^{-1} of the ground state.[25] Thus, one could expect
the changes in g factors of these ions in CaWO$_4$ and
LiYF$_4$ to be greatest for Dy^{3+}, next greatest for
Er^{3+}, lesser for Nd^{3+}, and least for Yb^{3+}. This
indeed is the case.

A strong superhyperfine structure (SHFS) was
found on all the resonances of the c-axis spectrum
for Yb^{3+}. The SHFS died out if the angle between
the external magnetic field and the c axis exceeded
2°, and the SHFS did not reappear in the plane per-
pendicular to the c axis. The c-axis SHFS on the
$I = 0$ line is displayed in Fig. 1. The 17-line spec-
trum is similar to the [100] SHFS spectrum seen
for CaF$_2$.[9] In that case the SHFS was attributed to
the interaction of the magnetic moments of the
nearest-neighbor fluorine nuclei with the paramag-
netic electrons of Yb^{3+}. The same mechanism may
be responsible for the SHFS of LiYF$_4$: Yb^{3+}.

VI. CONCLUSIONS

The EPR spectra of Nd^{3+}, Dy^{3+}, Er^{3+}, and Yb^{3+} have
been observed in LiYF$_4$. The spectra are attributed
to ions substituting for Y^{3+} which has tetragonal
(S_4) point symmetry in this scheelite crystal. The
axial spin Hamiltonian was diagonalized and least-
squares fit parameters were obtained. The g fac-
tors were used to determine that the ground states
of Nd^{3+} and Yb^{3+} were $\Gamma_{7,8}$ and $\Gamma_{5,6}$, respectively.
Superhyperfine structure was observed on the c-
axis spectrum of Yb^{3+}.

[1]I. N. Kurkin, Fiz. Tverd. Tela 8, 731 (1966) [Sov.
Phys. Solid State 8, 585 (1966)].

[2]L. Ya. Shekun, Opt. i Spektroskopiya 22, 422 (1967)
[Opt. Spectry. (USSR) 18, 417 (1965)].

[3]M. V. Eremin, I. N. Kurkin, O. I. Mar'yakhina, ana

L. Ya. Shekun, Fiz. Tverd. Tela 11, 2103 (1969) [Sov.
Phys. Solid State 11, 1967 (1970)].

[4]J. P. Sattler and J. Nemarich, Phys. Rev. B 1,
4249 (1970).

[5]E. A. Brown, J. Nemarich, N. Karayianis, and C. A.

Morrison, Phys. Letters 33A, 375 (1970).

[6]R. E. Thoma, C. F. Weaver, H. A. Friedman, H. Insley, L. A. Harris, and H. A. Yakel, Jr., J. Phys. Chem. 65, 1096 (1961).

[7]A. L. Harmer, A. Linz, and D. R. Gabbe, J. Phys. Chem. Solids 30, 1483 (1969).

[8]M. R. Brown, K. G. Roots, and W. A. Shand, J. Phys. C 2, 593 (1969).

[9]U. Ranon and J. S. Hyde, Phys. Rev. 141, 259 (1966).

[10]W. A. Shand, J. Crystal Growth 5, 143 (1969).

[11]H. E. Swanson, N. T. Gilfrick, and M. I. Cooke, Natl. Bur. Std. (U. S.) Circ. No. 539, 6 (1956); 7 (1957).

[12]A. Zalkin and D. H. Templeton, J. Chem. Phys. 40, 501 (1964).

[13]J. Leciejewicz, Z. Krist. 121, 158 (1965).

[14]K. Nassau and A. Broyer, J. Appl. Phys. 33, 3064 (1962); K. Nassau and G. M. Loiacono, J. Phys. Chem. Solids 24, 1503 (1963).

[15]U. Ranon and V. Volterra, Phys. Rev. 134, A1483 (1964).

[16]R. W. G. Wyckoff, Crystal Structures (Wiley, New York, 1965), Vol. 3.

[17]R. D. Shannon and C. T. Prewitt, Acta Cryst. B25, 925 (1969).

[18]E. A. Brown and J. Nemarich, Bull. Am. Phys. Soc. 16, 449 (1971).

[19]R. J. Elliott and K. W. H. Stevens, Proc. Roy. Soc. (London) A218, 553 (1953).

[20]N. Karayianis, J. Phys. Chem. Solids (to be published); D. E. Wortman, HDL Report No. TR-1554 (1971) (unpublished).

[21]I. V. Vasil'ev, G. M. Zverev, L. V. Makarenko, L. I. Plotkin, and A. I. Smirnov, Fiz. Tverd. Tela 11, 776 (1969) [Sov. Phys. Solid State 11, 625 (1969)]; I. N. Kurkin and E. A. Tsvetkov, Fiz. Tverd. Tela 11, 3610 (1969) [Sov. Phys. Solid State 11, 3027 (1970)].

[22]I. N. Kurkin, Fiz. Tverd. Tela 8, 731 (1966) [Sov. Phys. Solid State 8, 585 (1966)]; D. R. Mason, C. A. Morrison, C. Kikuchi, and R. T. Farrar, Bull. Am. Phys. Soc. 12, 468 (1967).

[23]A. A. Antipin, I. N. Kurkin, L. Z. Potvorova, and L. Ya. Shekun, Fiz. Tverd. Tela 7, 3685 (1965) [Sov. Phys. Solid State 7, 2979 (1966)].

[24]N. Karayianis (private communication).

[25]D. E. Wortman, J. Chem. Phys. (to be published).

Hyperfine Splitting of Er and Yb Resonances in Au: A Separation between the Atomic and Covalent Contributions to the Exchange Integral*

L. J. Tao, D. Davidov, R. Orbach, and E. P. Chock

Department of Physics, University of California, Los Angeles, California 90024

(Received 2 February 1971)

The hyperfine splitting has been observed in the magnetic resonance spectrum of dilute Au:Er and Au:Yb alloys. In both cases, the observed hyperfine coupling constant was larger (more positive) than in cubic nonmetallic hosts. Attributing this increase to conduction-electron polarization, and utilizing independent estimates of the $6s$ contribution to the hyperfine coupling constant, the atomic and covalent contributions to the localized-conduction-electron exchange integral are separated. It is found that the latter increases by an order of magnitude from Er to Yb in Au. This increase is attributed to the nearness of the $4f^{14}$ level to the Fermi surface in Au:Yb alloys, noting that Ag:Yb is diamagnetic.

I. INTRODUCTION

We report the first observation of the hyperfine splitting in the magnetic resonance spectrum of dilute Au:Yb and Au:Er alloys. In both cases the hyperfine coupling constant A is larger (more positive) than in nonmetallic hosts with the same local symmetry. This increase is attributed to the spin-polarized conduction electrons. The temperature dependence of the resonance linewidth yields values for the localized–conduction-electron exchange coupling constant J. Knowing the increase in A and J over the insulator value, and using the estimate of Gossard et al.[1] of the value of the $6s$ contribution to the hyperfine coupling constant, we are able to separate out the two contributions to J, commonly referred to as "atomic" (J_{at}) and "covalent mixing"

(J_{cm}), for both alloys. We find the ratio of $(J_{cm})_{Au:Yb}$ to $(J_{cm})_{Au:Er}$ to be approximately 20, much larger than expected from simple theoretical estimates.[2] We speculate, knowing that the isomorphic alloy Ag:Yb is diamagnetic,[3] that this is caused by a close proximity of the $4f^{14}$ virtual level in Au:Yb to the Fermi level, allowing a strong "absorption" contribution[2] to J_{cm} to obtain for that alloy.

II. EXPERIMENTAL RESULTS

A. Au:Er

The magnetic resonance spectra of powdered samples of Au:Er for Er concentrations of 50, 100, 500, 1000, and 5000 ppm was obtained as a function of temperature. The measurements were conducted at 3-cm wavelength, the apparatus having been described elsewhere.[4] The spectrum of a 50-ppm